Supporting Information

Self-Assembly and -Cross-Linking Lamellar Films by Nanophase Separation with Solvent-Induced Anisotropic Structural Changes

Kohei Amada[†], Manabu Ishizaki[‡], Masato Kurihara[‡] and Jun Matsui[‡]*

[†]Graduate School of Science and Engineering, [‡]Faculty of Science Yamagata University, 1-4-12 Kojirakawa -machi, Yamagata 990-8560, Japan

Table S1. Synthesis condition of copolymer and composition, molecular weight, polydispersity and thermal property

run	copolymer	molar ratio DDA/TMSPA in feed	molar ratio DDA/TMSPA in product	M_n / 10^4	M_w/M_n	T_g / ˚C	T_M / ˚C	T_{5d} / ˚C
1	p(DDA/TMSPA13) [a)]	74 : 26	87 : 13	2.52	2.06	39.6	-37.8	328

a) Polymerized at 60 °C for 12 h.

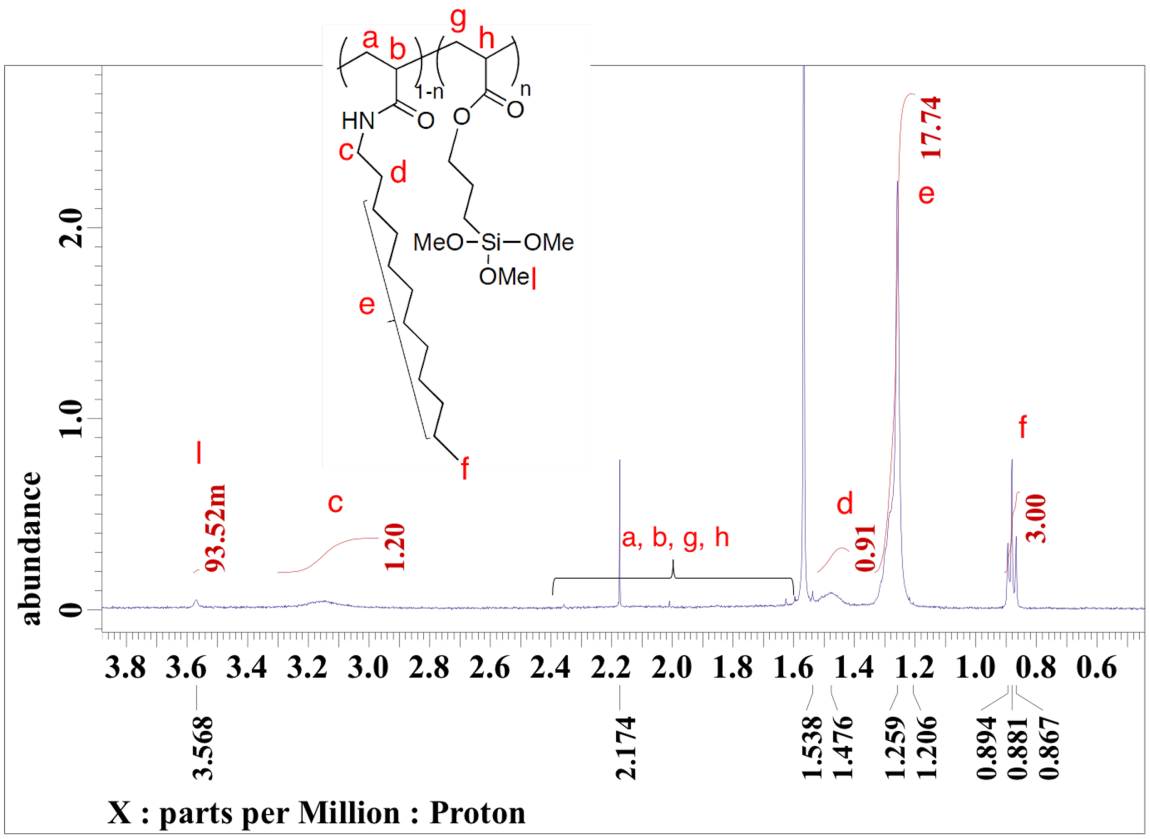

Figure S1. ^{1}H NMR spectrum of p(DDA/TMSPA1).

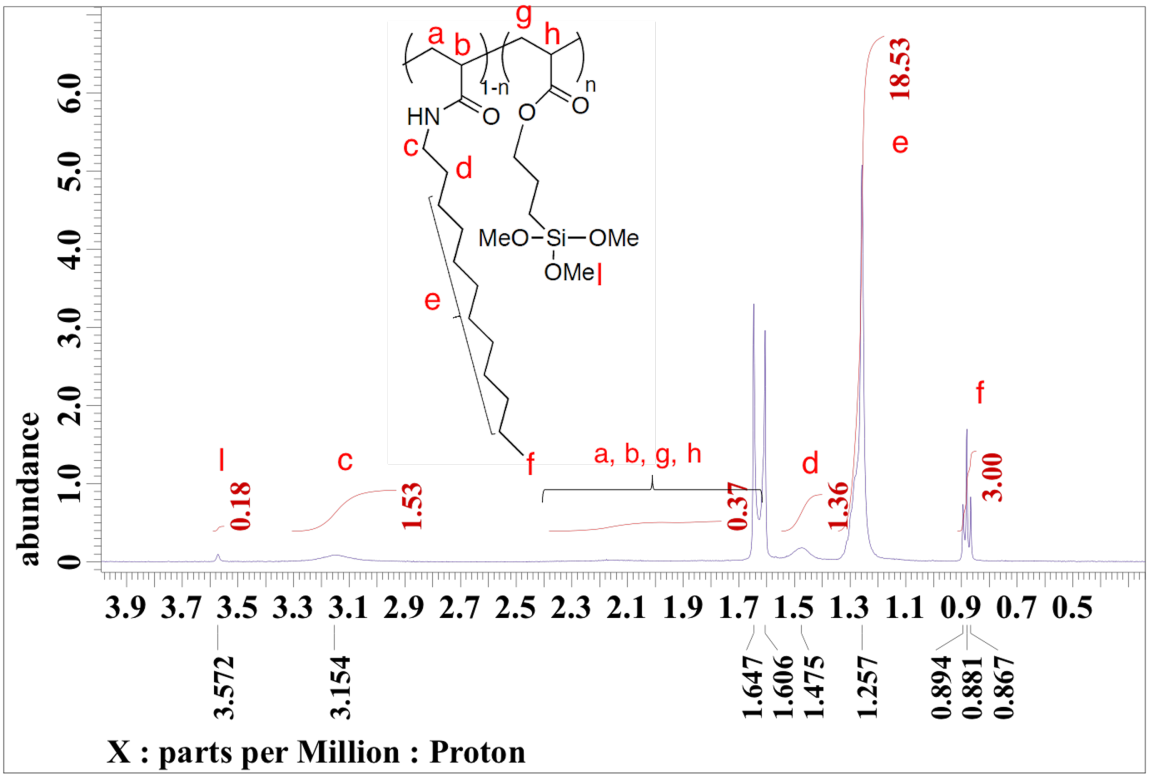

Figure S2. ^{1}H NMR spectrum of p(DDA/TMSPA2).

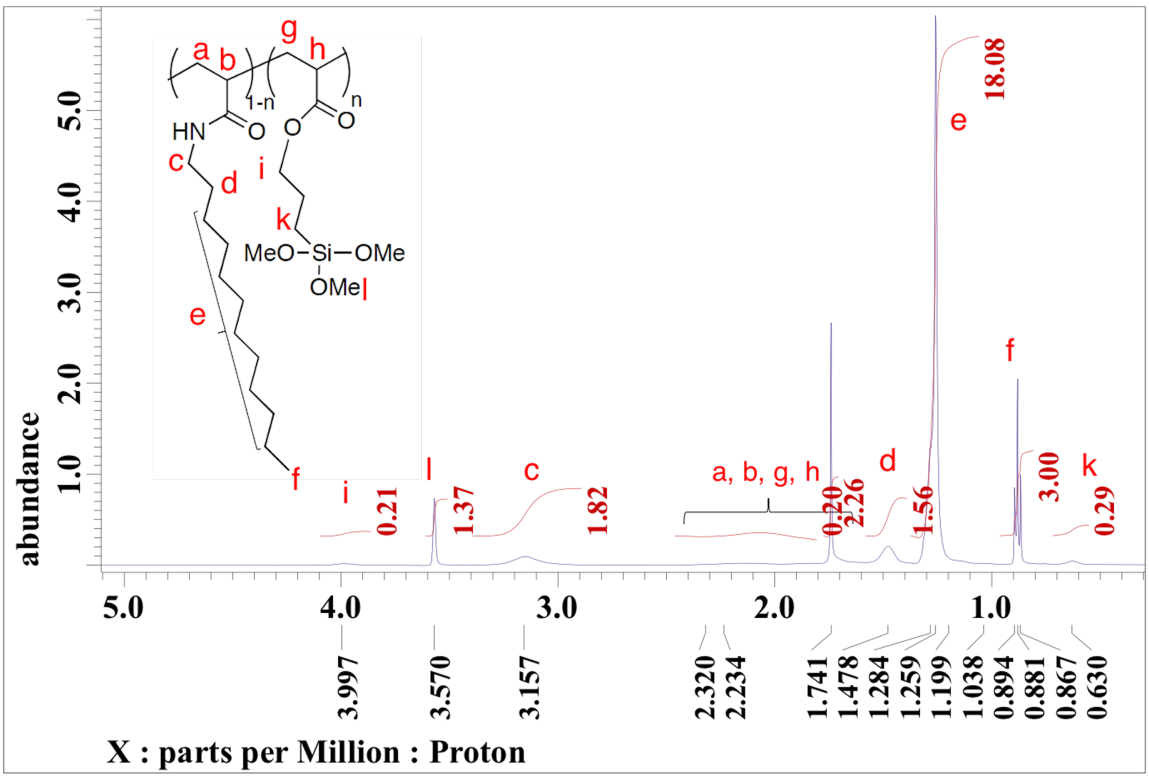

Figure S3. ^{1}H NMR spectrum of p(DDA/TMSPA13).

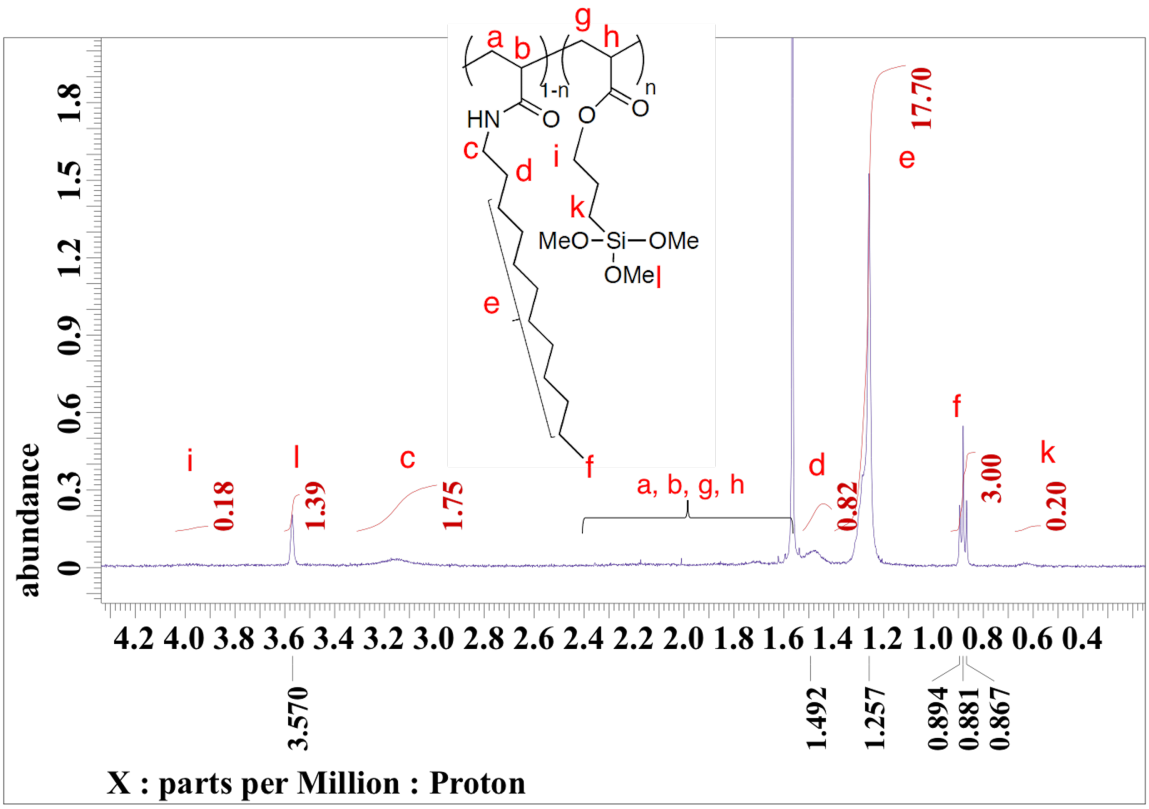

Figure S4. ^{1}H NMR spectrum of p(DDA/TMSPA13) synthesized by run 1 of Table S1.

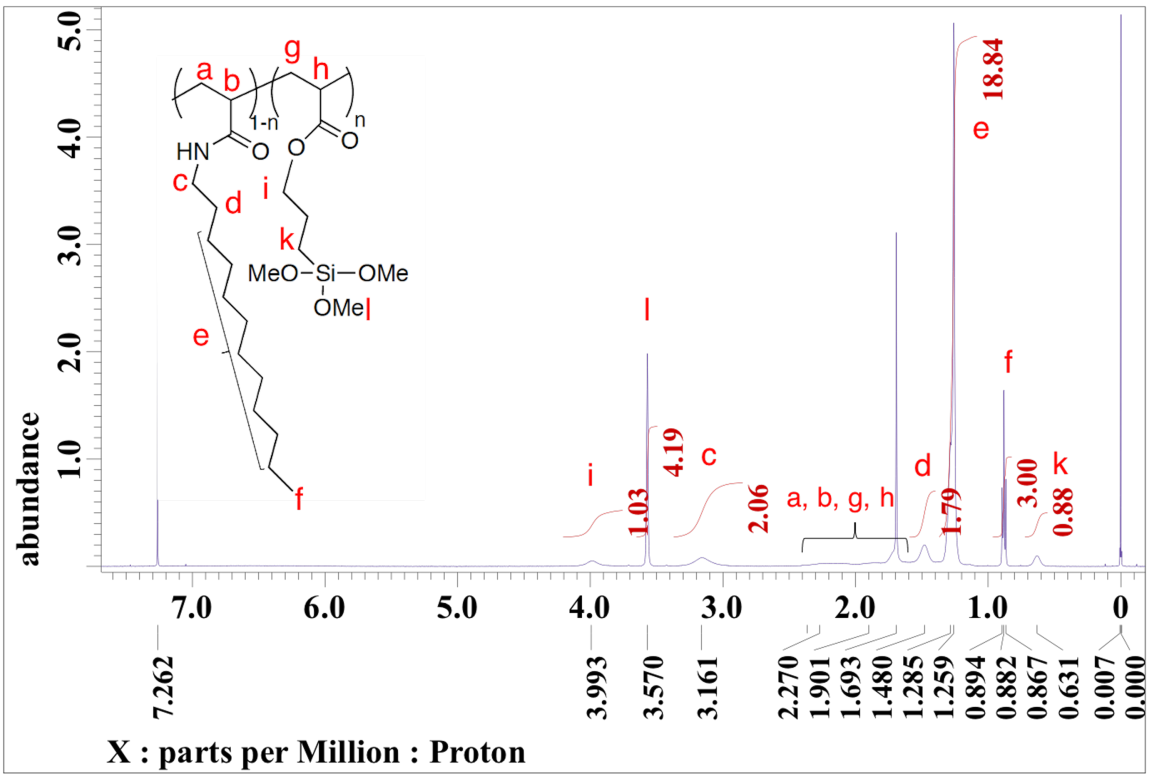

Figure S5. ^{1}H NMR spectrum of p(DDA/TMSPA32).

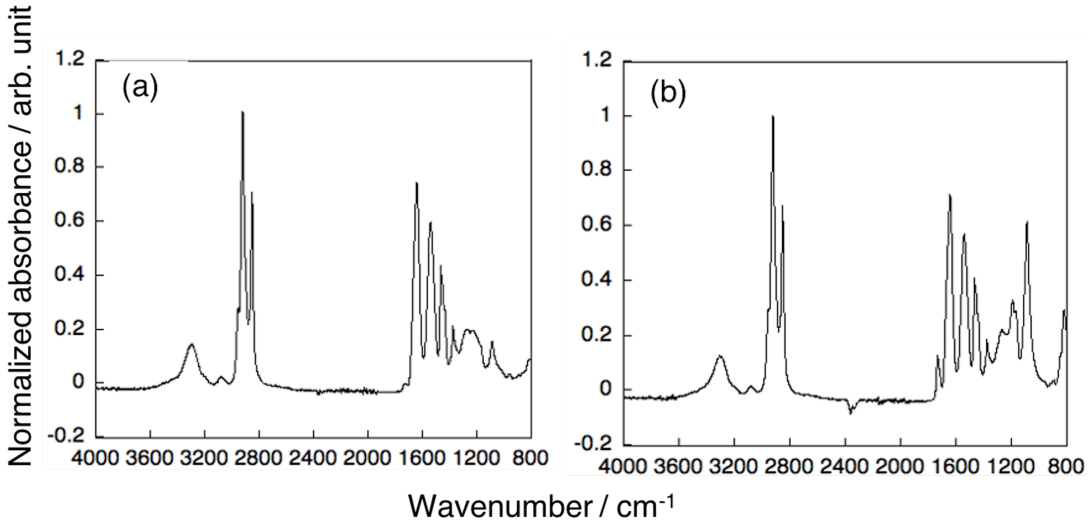

Figure S6. FT-IR spectra of (a) p(DDA/TMSPA2) and (b) p(DDA/TMSPA13). The spectra were normalized using the asymmetric stretching vibration of CH_2.

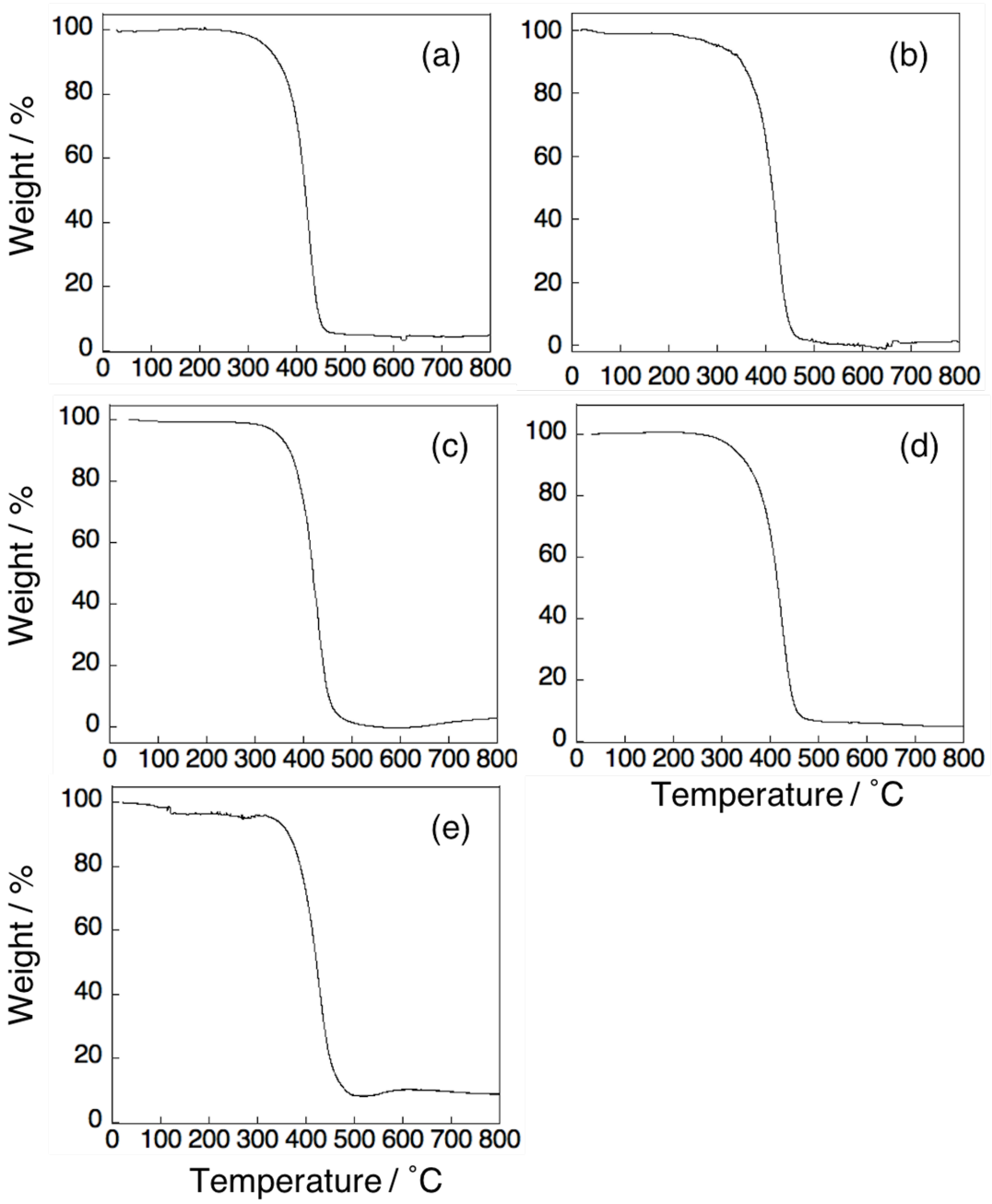

Figure S7. TGA curves of p(DDA/TMSPA) at a heating rate of 10 ˚C min^{-1} under nitrogen atmosphere. (a) p(DDA/TMSPA1), (b) p(DDA/TMSPA2), (c) p(DDA/TMSPA13), (d) p(DDA/TMSPA13) which was run 1 of Table S1 and (e) p(DDA/TMSPA32).

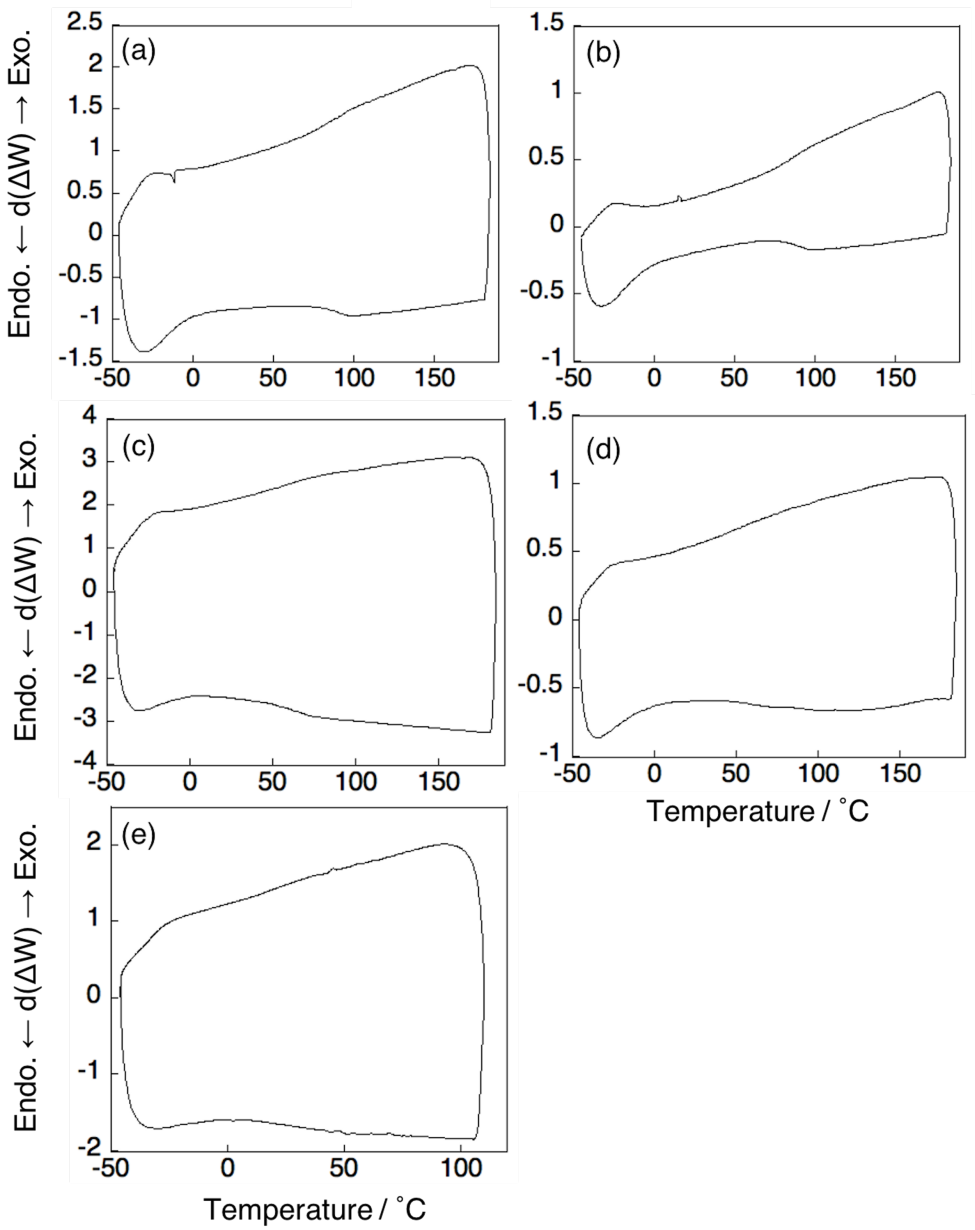

Figure S8. DSC curves of p(DDA/TMSPA) for the third heating and cooling process at a rate of 10 ºC min^{-1} under nitrogen atmosphere. (a) p(DDA/TMSPA1), (b) p(DDA/TMSPA2), (c) p(DDA/TMSPA13), (d) p(DDA/TMSPA13) which was run 1 of Table S1 and (e) p(DDA/TMSPA32).

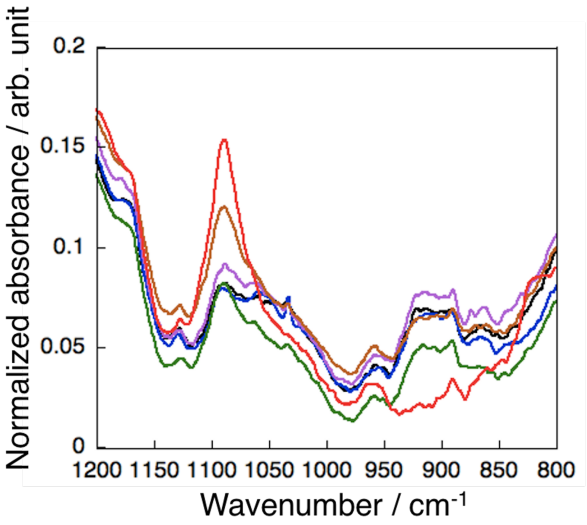

Figure S9. Normalized FT-IR spectra of p(DDA/TMSPA2) powder. Before humid annealing (red), humid annealed for 24 h (brown), 48 h (green), 72 h (purple), 96 h (blue) and 120 h (black). The spectra were normalized using the asymmetric stretching vibration of CH_2.

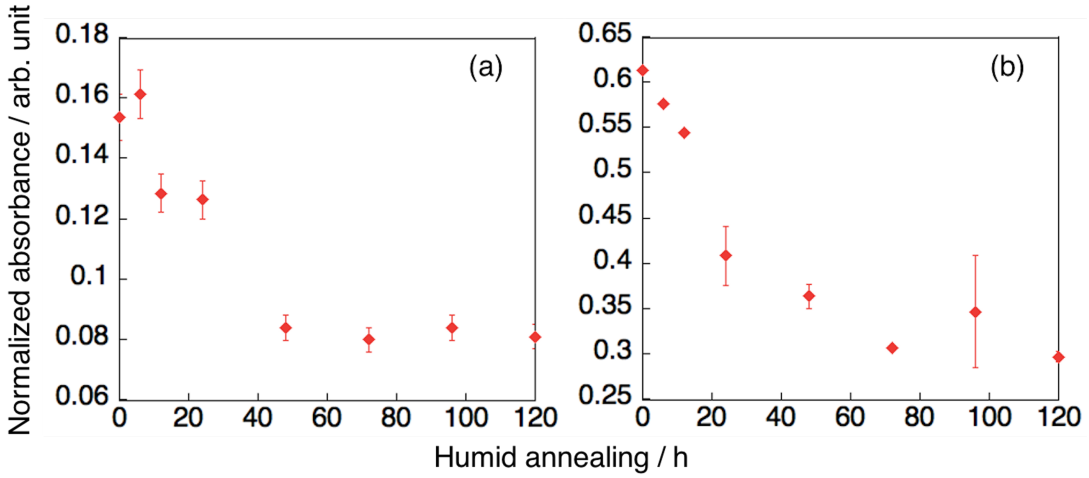

Figure S10. Plots for normalized absorbance of Si-OMe as humid annealing time. (a) p(DDA/TMSPA2) and (b) p(DDA/TMSPA13) powders. The absorbance was normalized using the asymmetric stretching vibration of CH_2.

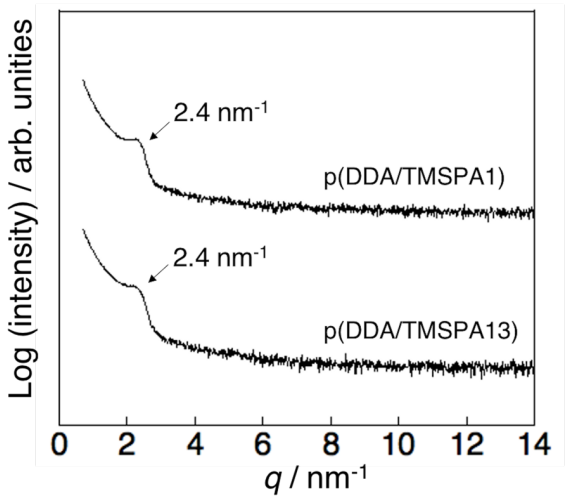

Figure S11. XRD patterns of p(DDA/TMSPA1) (top) and p(DDA/TMSPA13) (bottom) thin films annealed at 60 ˚C for 24 h.

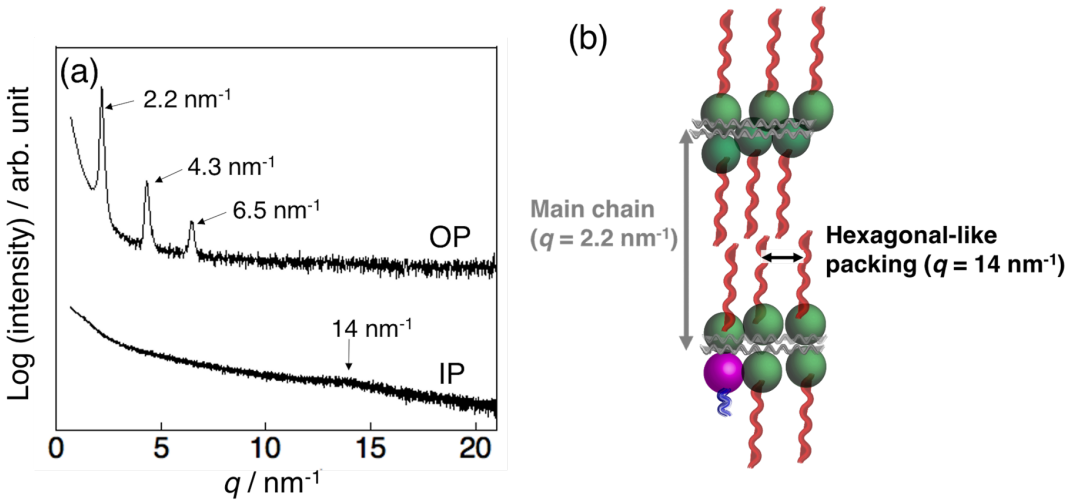

Figure S12. (a) XRD patterns of p(DDA/TMSPA13) thin film humid annealed at 60 ˚C for 96 h. In the figure, the top and bottom pattern are the pattern measured in the out-of-plane and in-plane direction, respectively. (b) Schematic image of the lamellar structure of thin films of p(DDA/TMSPA). The diffraction of short axis side of dodecyl side chains assign as hexagonal-like packing.

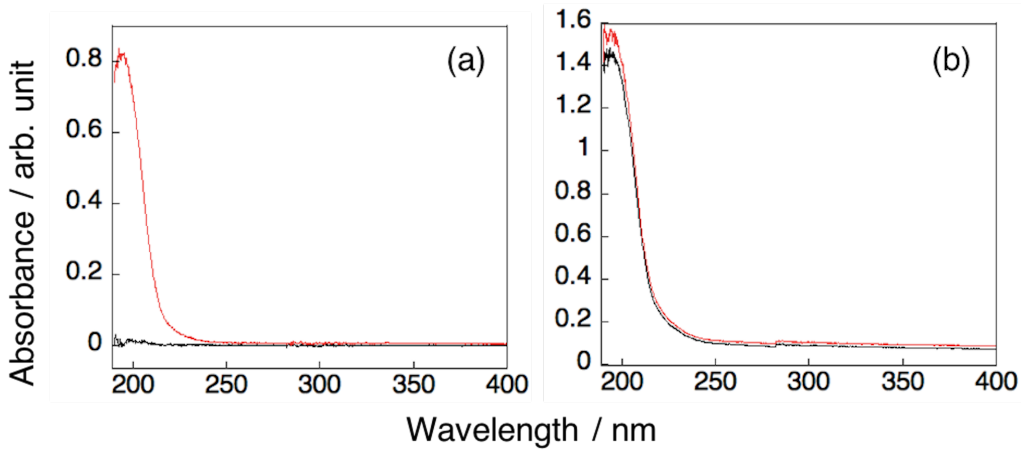

Figure S13. UV-vis spectra of humid-annealed p(DDA/TMSPA) thin films before (red) and after (black) dipping into toluene. (a) p(DDA/TMSPA2) and (b) p(DDA/TMSPA13) thin films.

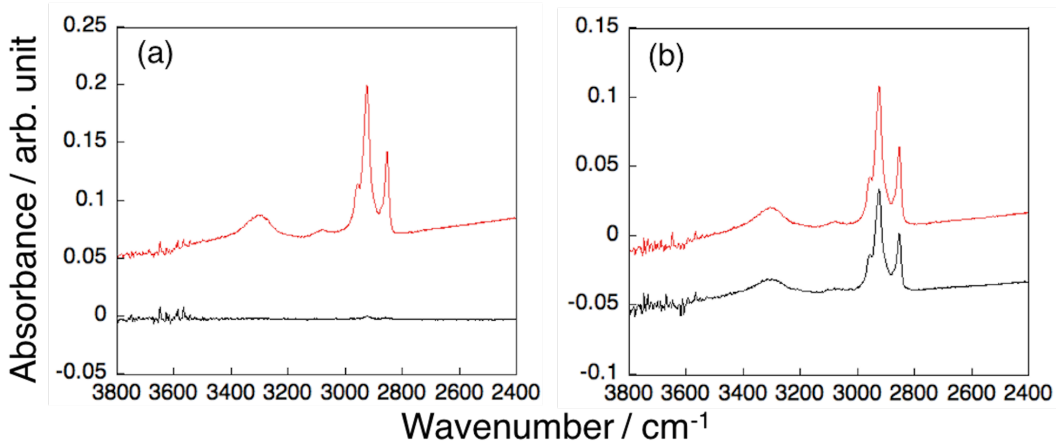

Figure S14. FT-IR spectra of humid annealed p(DDA/TMSPA) thin films before (red) and after (black) dipping into toluene. (a) p(DDA/TMSPA2) and (b) p(DDA/TMSPA13) thin films.

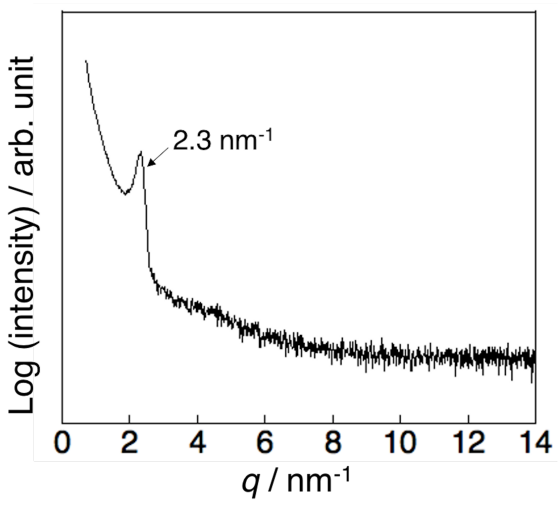

Figure S15. XRD pattern for toluene dipped p(DDA/TMSPA13) thin films followed by annealed at 60 ˚C for 24 h.

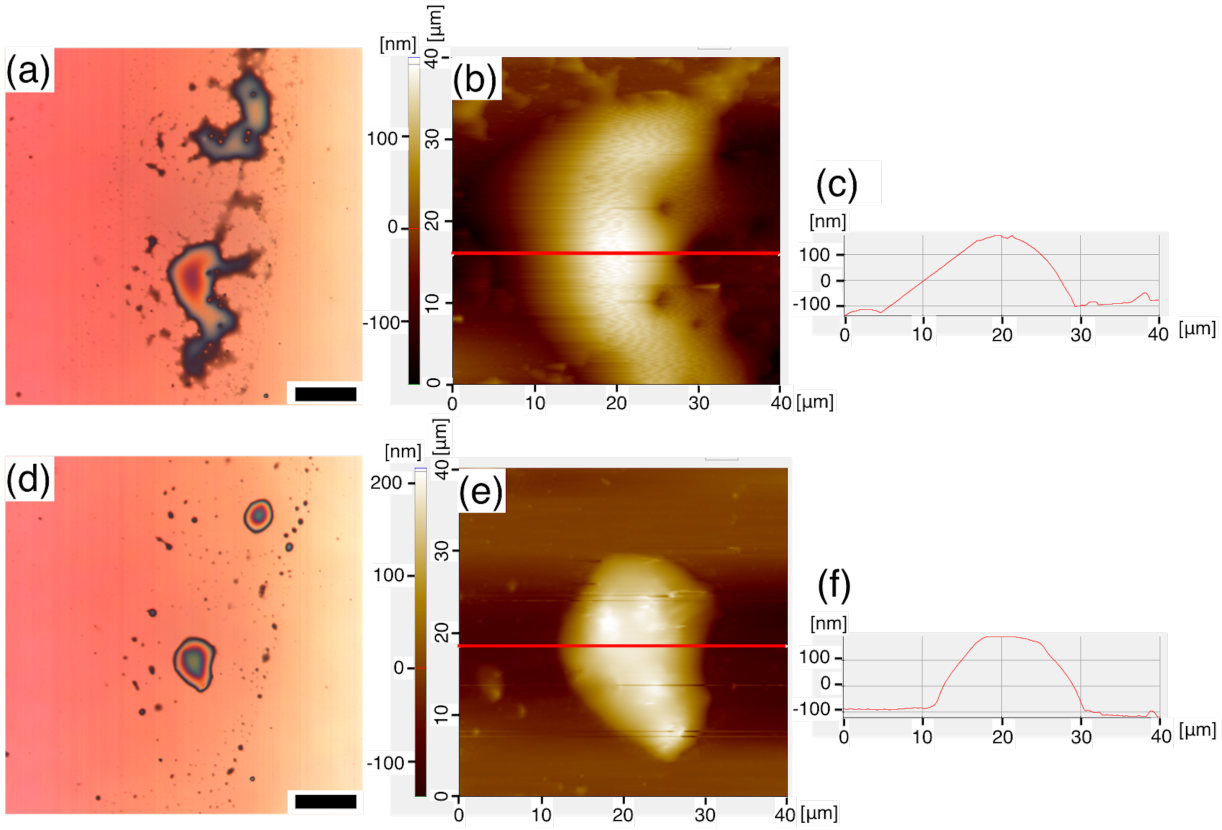

Figure S16. LM images and AFM topological images of p(DDA/TMSPA13) films before (a,b) and after (d,e) humid annealing; (c,f) represent the line profiles for (b,e), respectively. (Scale bar: 25 µm).